Int. J. Mol. Sci. **2015**, *16*, 350-362; doi:10.3390/ijms16010350

OPEN ACCESS
International Journal of
Molecular Sciences
ISSN 1422-0067
www.mdpi.com/journal/ijms

Article

Stable Hydrogen Production from Ethanol through Steam Reforming Reaction over Nickel-Containing Smectite-Derived Catalyst

Hiroshi Yoshida, Ryohei Yamaoka and Masahiko Arai *

Division of Chemical Process Engineering, Faculty of Engineering, Hokkaido University, Sapporo 060-8628, Japan; E-Mails: yoshida@chem.kumamoto-u.ac.jp (H.Y.); yamaoka.ryouhei@kao.co.jp (R.Y.)

* Author to whom correspondence should be addressed; E-Mail: marai@eng.hokudai.ac.jp; Tel./Fax: +81-(0)11-706-6594.

Academic Editor: Andreas Taubert

Received: 25 November 2014 / Accepted: 18 December 2014 / Published: 25 December 2014

Abstract: Hydrogen production through steam reforming of ethanol was investigated with conventional supported nickel catalysts and a Ni-containing smectite-derived catalyst. The former is initially active, but significant catalyst deactivation occurs during the reaction due to carbon deposition. Side reactions of the decomposition of CO and CH_4 are the main reason for the catalyst deactivation, and these reactions can relatively be suppressed by the use of the Ni-containing smectite. The Ni-containing smectite-derived catalyst contains, after H_2 reduction, stable and active Ni nanocrystallites, and as a result, it shows a stable and high catalytic performance for the steam reforming of ethanol, producing H_2.

Keywords: hydrogen; steam reforming; ethanol; nickel; smectite

1. Introduction

Fuel cells have been given attention as a clean technology for energy, and hydrogen is one of the most promising fuels due to many advantages, such as high energy efficiency, no emission of air pollutants and greenhouse gases and the presence of abundant H_2-containing resources [1,2]. However, at present, hydrogen is mainly produced from fossil fuels by steam reforming of natural gas and light oil, and so, new and sustainable ways for hydrogen production are greatly required. Hydrogen production from

biomass is an ideal means, and many researchers have investigated the steam reforming of ethanol, which can be produced by the fermentation of biomass [3–13]. Only CO_2 and H_2 are theoretically produced through steam reforming of ethanol (Equation (1)), but in practice, some other reactions can also occur and several intermediates and by-products formed. The steam reforming of ethanol (Equation (1)) mainly proceeds through several consecutive reactions (Equations (2)–(5)) [6]. A number of metal-supported catalysts have been investigated using nickel [3–6], cobalt [8–10] and noble metals [11–14], and low-cost nickel-based catalyst showed the highest catalytic performance among the transition metals examined so far.

$$C_2H_5OH + 3H_2O \leftrightarrow 2CO_2 + 6H_2 \quad (1)$$

$$C_2H_5OH \leftrightarrow CH_3CHO + H_2 \quad (2)$$

$$CH_3CHO \leftrightarrow CH_4 + CO \quad (3)$$

$$CH_4 + 2H_2O \leftrightarrow CO_2 + 4H_2 \quad (4)$$

$$CO + H_2O \leftrightarrow CO_2 + H_2 \quad (5)$$

When Ni-based catalyst is used for the steam reforming of ethanol, the main problem is a catalyst deactivation by carbon deposition formed from several side reactions. Ethylene is formed by the dehydration of ethanol (Equation (6)); it is rapidly reduced to carbon species, which deposit on the catalyst (Equation (7)). The decomposition of methane (Equation (8)) and the Boudouard reaction (Equation (9)) also occur and cause the catalyst activity of Ni to decrease; hence, the suppression of these side reactions and carbon deposition is one of the most significant problems for the development of practical Ni-based catalysts for the steam reforming of ethanol.

$$C_2H_5OH \leftrightarrow C_2H_4 + H_2O \quad (6)$$

$$C_2H_4 \rightarrow 2C + 2H_2 \quad (7)$$

$$CH_4 \rightarrow C + 2H_2 \quad (8)$$

$$2CO \rightarrow C + CO_2 \quad (9)$$

Christensen *et al.* [15] used hydrotalcite as a support of Ni catalyst for the steam reforming of methane and investigated the influence of the crystallite size of Ni. They reported that a smaller Ni crystallite has higher resistance to coke formation compared to conventional Ni-supported catalysts. Muroyama *et al.* [6] prepared a Ni-containing material of $NiAl_2O_4$ and showed its high catalytic performance and stability. These studies suggest that the modification of the structure around Ni species is a key to the development of durable Ni catalysts with less carbon deposition. In the present work, a Ni-containing mesoporous smectite material has been synthesized and used as a precursor of Ni catalyst, which has been prepared through a certain reduction. For a comparison, another smectite material containing Mg was prepared and used as a support for Ni, which was loaded by impregnation. A few other conventional supported Ni catalysts were also prepared. The catalytic performance and durability in the steam reforming of ethanol were examined and compared for various Ni catalysts, including the smectite-derived and conventional supported Ni catalysts.

Smectite is one of the layered clay minerals, and it can be synthesized by a simple hydrothermal method [16]. There is a layer consisting of one octahedral sheet sandwiched by two tetrahedral sheets,

and it is possible to introduce divalent or trivalent cations, such as Mg^{2+}, Zn^{2+}, Al^{3+} and Fe^{3+} in a framework of an octahedral sheet by using different precursors. The synthetic smectite materials can serve as catalysts and supports due to their high surface area and their flexible structural features, as demonstrated by a number of studies, including hydrogenation [17,18], hydrogenolysis [18], synthesis of dimethyl carbonate [19], transesterification and Knoevenagel reactions [20], steam reforming of acetic acid [21], dry reforming of methane with carbon dioxide [22], selective methanation of carbon monoxide [23] and others [24,25]. The metal species in the smectite structure may be reduced, move to the surface layer and form metal clusters/crystallites on the wall of pores through heat treatment with H_2, which can thus serve as dispersed metal catalysts. These morphological features of metal-containing smectite-derived materials may give some beneficial effects to the synthesis of Ni catalysts for the steam reforming of ethanol, as well. Therefore, the present work has been undertaken to improve the activity and durability of Ni-based catalysts by using Ni-containing smectite-derived materials as catalyst precursors.

2. Results and Discussion

The Mg- and Ni-containing smectite samples are abbreviated as SM and SM(Ni) (or SM(Ni35) to indicate the Ni content), respectively, in this work. Table 1 shows the textual properties of Ni catalysts prepared (after reduction at 600 °C), including SM(Ni35), a smectite-derived material containing Ni in 35 wt % (Entry 1), and other supported Ni catalysts prepared by impregnation using different supports and/or different Ni loadings (Entries 2–7). Among the catalysts prepared, SM(Ni35) gave the highest surface area of 493 $m^2 \cdot g^{-1}$, and its Ni crystallite size of 5.4 nm was the smallest among the samples with the same Ni loading (Entries 1, 4–7). However, its CO uptake was 30.5 $\mu mol \cdot g^{-1}$, which was smaller than 41.0 $\mu mol \cdot g^{-1}$ for Ni35/SM, meaning that the amount of exposed surface Ni sites in the SM(Ni35) was smaller in spite of its smaller Ni crystallite size (Entries 1, 4). These results indicate that some Ni species in SM(Ni35) remain in the framework of the smectite structure even after reduction. Generally, the crystallite size of supported metal tends to increase with the metal loading, as shown in the case of Ni/SM (Entries 2–4), and so, it is difficult to synthesize metal nanoparticles in a high metal loading. However, in the present case of Ni-containing smectite-derived material, the crystallite size of Ni was smaller than those of the Ni catalysts impregnated in smaller loadings, Ni05/SM and Ni10/SM (Entries 1–3). Hence, the Ni nanoparticle was able to be produced in a high metal loading when a smectite-derived material was used as a starting precursor.

Table 1. Textual properties of the different Ni catalysts prepared.

Entry	Catalyst	Ni Loading (wt %)	Surface Area ($m^2 \cdot g^{-1}$)	CO Uptake [a] ($\mu moL \cdot g^{-1}$)	d_{Ni} [b] (nm)
1	SM(Ni35)	35	493	30.5	5.4
2	Ni05/SM	5	478	2.4	6.6
3	Ni10/SM	10	457	7.3	7.5
4	Ni35/SM	35	293	41.0	21.0
5	Ni35/MgO	35	25	23.8	19.0
6	Ni35/SiO_2	35	323	20.2	37.0
7	Ni35/Al_2O_3	35	100	35.9	22.0

[a] The amount of CO adsorbed on the catalyst measured by CO chemisorption; [b] crystallite size of the Ni particle calculated from XRD results.

The formation of Ni nanoparticles in SM(Ni35) was examined by XRD (Figure 1). Two peaks assigned to the Ni metal were seen for SM(Ni35) after reduction, whereas no peak was observed before reduction (Figure 1a,b), indicating that Ni species were contained in a framework of SM(Ni35) just after synthesis, and these moved to the surface during the reduction process, forming nanoparticles. On the other hand, sharp peaks assigned to NiO were observed for Ni35/SM before reduction (Figure 1d) and changed almost to Ni metal after reduction (Figure 1e) with no change in the Ni crystallite size. Therefore, there are different mechanisms for the formation of Ni nanoparticle on SM(Ni35) and in Ni35/SM. For SM(Ni35), Ni species in a framework moved to the surface during reduction, but a strong interaction between Ni and the framework inhibited the significant sintering of Ni species, resulting in the formation of small Ni nanoparticles. For Ni35/SM, the crystallite size of Ni was determined before the reduction process, which was likely to depend on the calcination conditions.

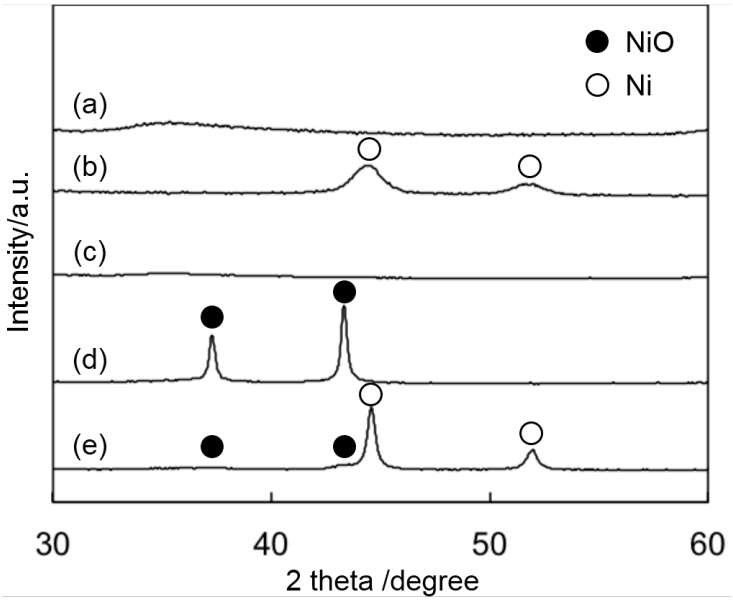

Figure 1. XRD patterns of SM(Ni35) before reduction (a) and after reduction (b); SM after calcination (c); Ni35/SM before reduction (d) and after reduction (e).

2.1. Catalytic Activity of Smectite-Derived and Conventional Supported Ni Catalysts

Steam reforming of ethanol was carried out at 500 °C over the Ni catalysts prepared, which were compared to the total conversion and H_2 yield at the initial stage (after 5 min) and at the later stage (after 200 min) (Figure 2). For a comparison, the catalytic performance of SM support was also measured. At the initial stage, a supported Ni catalyst of Ni35/SM gave the highest catalytic performance in both ethanol conversion and H_2 yield among the catalysts used, but a remarkable catalyst deactivation was observed after 200 min. For the smectite-derived SM(Ni35) catalyst, however, initial conversion and H_2 yield were lower than those of Ni35/SM, but, at the later stage of the reaction, higher catalytic performance was obtained despite the lower amount of surface Ni sites determined by CO chemisorption (Entries 1, 4 in Table 1). These results indicate that the durability of the Ni catalyst was improved by using a Ni-containing smectite as a precursor. After 200 min of reaction, the highest H_2 yield was achieved over SM(Ni35) catalyst. It should be mentioned that an Al_2O_3-surpported catalyst of Ni35/Al_2O_3 gave a high conversion even after a long-time reaction, but the main carbon-containing product changed

from CO_2 to ethylene, which should be produced by the dehydration of ethanol on the acid sites of Al_2O_3 support, but not on Ni particles. Namely, undesired side reactions occurred, and so, Ni35/Al_2O_3 was losing its activity for the desired H_2 production by the steam reforming of ethanol, as shown in Figure 2. The total ethanol conversion and H_2 yield were plotted against the amount of exposed Ni sites measured by CO chemisorption in Figure 3. A clear correlation between the amount of surface Ni and either conversion or H_2 yield was observed at the initial stage, meaning that the initial reaction rate simply depended on the amount of active sites, and these catalysts lost their activity after 200 min of reaction to a similar extent (Figure 3a). However, the extent of catalyst deactivation was relatively lower in the case of using SM(Ni35) compared with the other catalysts prepared by impregnation. That is, the durability of the catalyst was improved by using the Ni-containing smectite as the precursors.

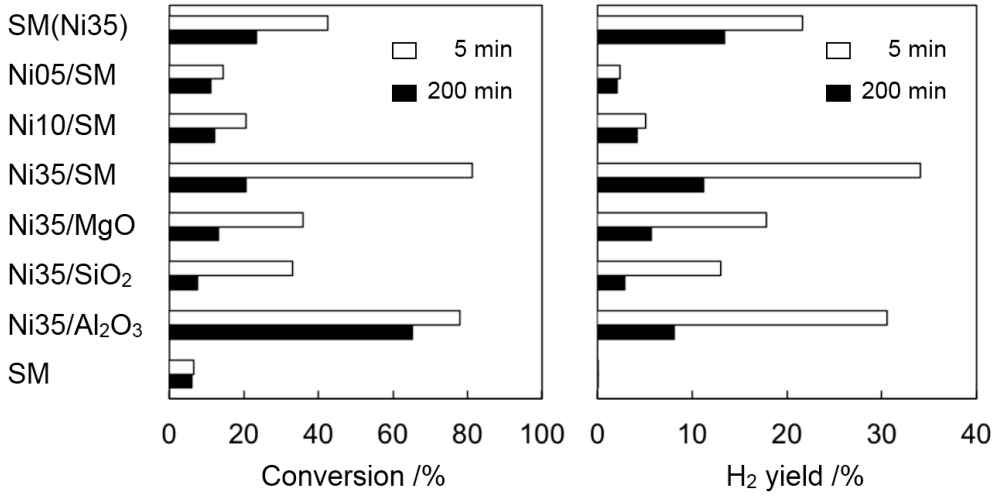

Figure 2. Total conversion and H_2 yield for steam reforming of ethanol over different Ni catalysts at 500 °C after 5 min (□) and 200 min (■).

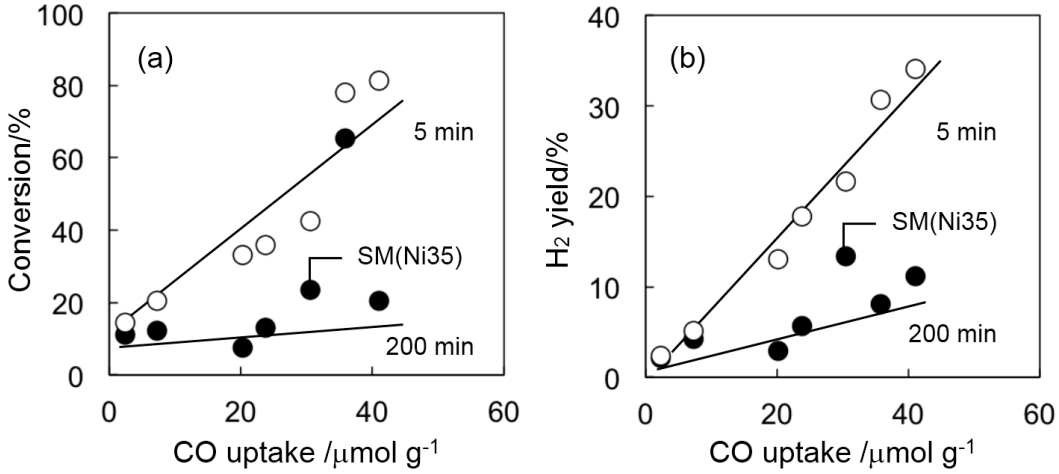

Figure 3. Relationship between the amount of surface Ni (CO uptake measured by CO chemisorption) and either total conversion (**a**) or H_2 yield (**b**) after the reaction time of 5 min (○) and 200 min (●).

2.2. Catalyst Deactivation

XRD results for Ni35/SM and SM(Ni35) catalysts after reaction showed the peak at 26°, which was assignable to carbon deposition (Figure 4). On the other hand, the crystallite size of Ni particles determined by XRD did not change, as shown in Figure 4, indicating that the sintering of Ni was unlikely to occur under the present reaction conditions. Therefore, we conclude that the carbon deposition was the main cause of the catalyst deactivation. Carbon deposition was observed for all Ni catalysts used, and the amounts of the carbon deposited were determined from the total amount of CH_4 detected during H_2 heat treatment. Interestingly, the amount of carbon deposition per Ni surface area tended to decrease with the decreasing crystallite size of Ni particles (Figure 5), meaning that the formation of the Ni nanoparticle not only results in the increase of exposed Ni surface area, but also contributes to the decrease of the carbon deposition.

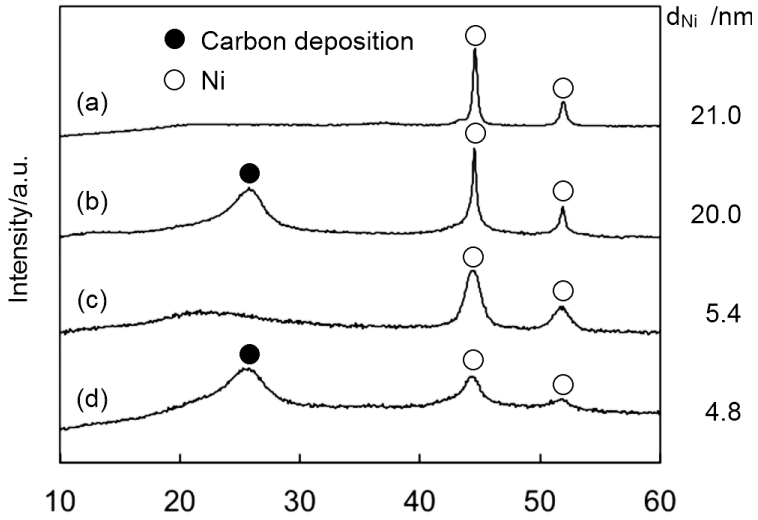

Figure 4. XRD patterns and the crystallite sizes of Ni35/SM before (a) and after reaction (b); and SM(Ni35) before (c) and after reaction (d) at 500 °C for 6 h.

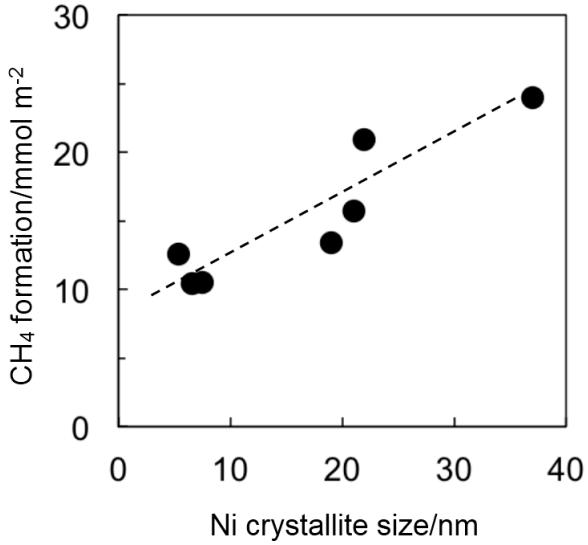

Figure 5. Relationship between the crystallite size of Ni particles and the amount of CH_4 formed (the amount of carbon deposits) per exposed Ni surface area.

Figure 6 gives the time profiles of the total conversion and H_2 yield over SM(Ni35) and other Ni-loaded catalysts prepared by impregnation. For the Ni35/SM catalyst, remarkable catalyst deactivation was observed within a first 100 min, and the deactivation continued to occur gradually after 100 min. Such catalyst deactivation was not observed for Ni05/SM and Ni10/SM, which have small Ni nanoparticles, as shown in Table 1, implying that a rapid catalyst deactivation due to carbon deposition is unlikely to occur on a small Ni nanoparticle. For SM(Ni35), the formation of Ni nanoparticle in SM(Ni35) may be responsible for its relatively stable catalytic performance for both conversion and H_2 yield during the reaction.

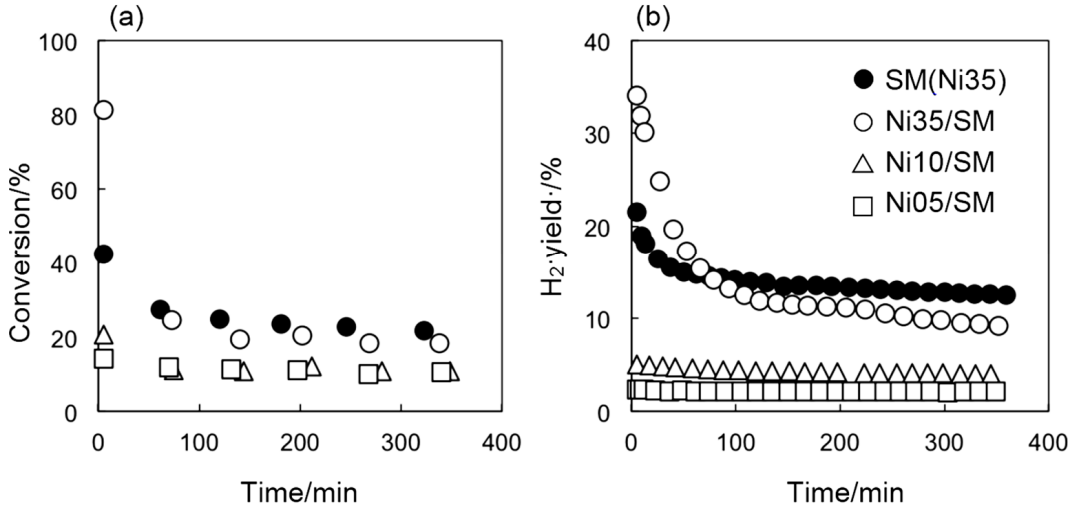

Figure 6. Time profiles of total conversion (**a**) and H_2 yield (**b**) over different Ni catalysts at 500 °C.

Time profiles of the product selectivity were examined to further discuss the carbon deposition (Figure 7). At the beginning of the reaction over SM(Ni35) and Ni35/SM, high selectivity to CO and CH_4 (Figure 7b,c) and low selectivity to CH_3CHO and CO_2 (Figure 7a,e) were obtained; the dehydrogenation of ethanol to C_1 species (Equation (2)) and the decomposition of CH_3CHO (Equation (3)) took place rapidly, but further reaction of C_1 species with water, the steam reforming of CH_4 (Equation (4)) and the water gas shift reaction (Equation (5)) should be slower than the former reactions. During the reaction, the selectivity to CH_3CHO and CO_2 tended to increase (Figure 7a,e) while that to CO and CH_4 decreases (Figure 7b,c), implying that the decomposition of CH_3CHO to CO and CH_4 (Equation (3)) was suppressed by carbon deposition compared with the other reactions. Therefore, one can say that CO and CH_4 formed from CH_3CHO induced the side reactions to form the carbon deposition on the catalyst (Equations (8) and (9)), which suppressed the further decomposition of CH_3CHO and resulted in the catalyst deactivation. Vicente *et al.* [26,27] investigated the steam reforming of ethanol over Ni/SiO_2 catalyst, and they noted that CO and CH_4 formed by the decomposition of CH_3CHO were the precursors of the filamentous coke deposited on the Ni surface. For the three catalysts prepared by impregnation, the selectivity to CO against that to CH_4 was higher, and this means that the rate of CH_4 steam reforming is faster than the water gas shift reaction. For the smectite-derived SM(Ni35) catalyst, however, the selectivity to CO against that to CH_4 was relatively lower compared with the case of Ni35/SM, which indicates that the reactivity of CO was enhanced by Ni nanoparticles in the framework of the smectite structure.

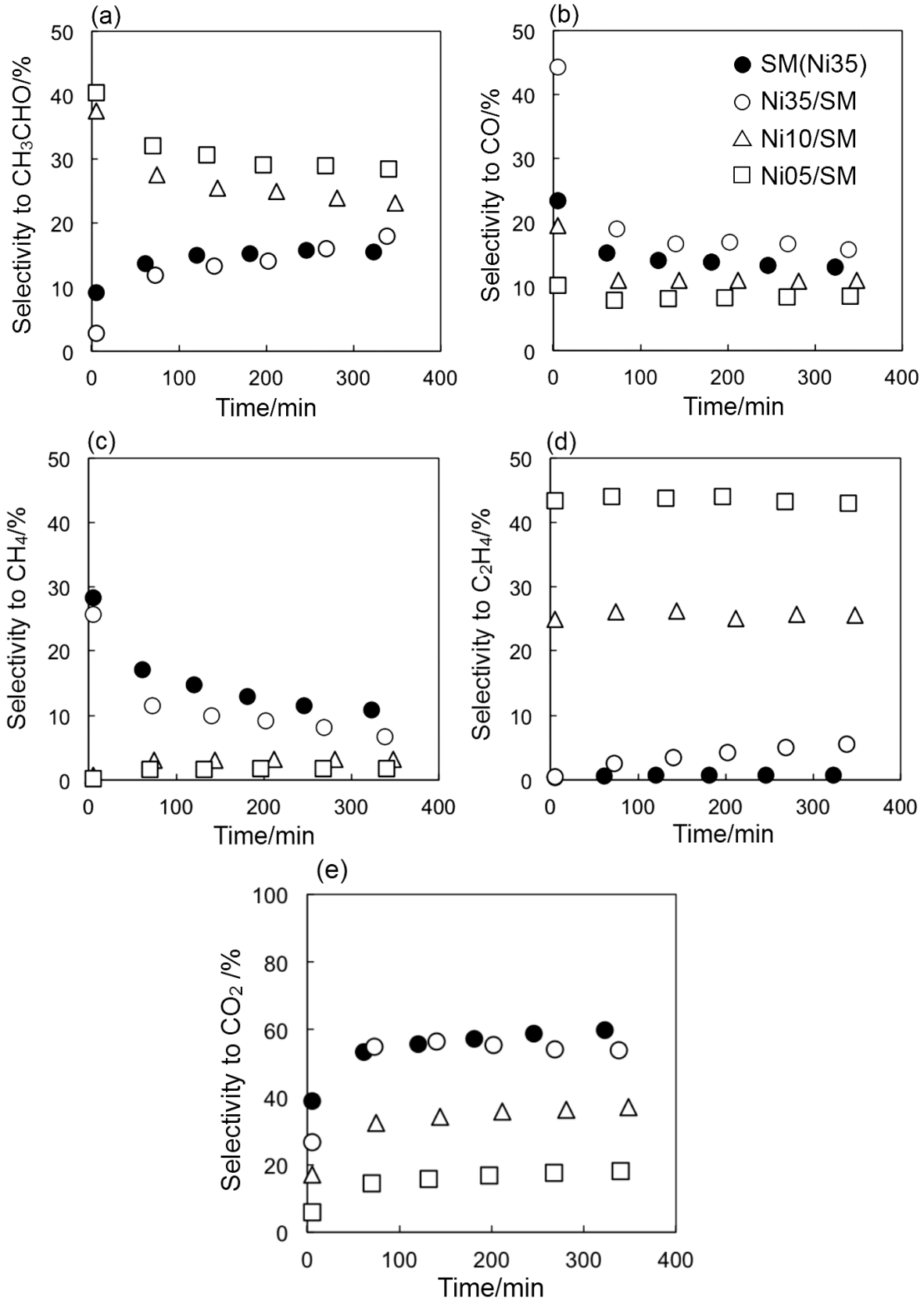

Figure 7. Time profiles of selectivity to CH_3CHO (**a**); CO (**b**); CH_4 (**c**); C_2H_4 (**d**) and CO_2 (**e**) over different Ni catalysts given at 500 °C.

It is known that the decomposition of C_2H_4 also causes carbon deposition (Equation (7)). The formation of C_2H_4 was observed for the catalysts prepared by impregnation, but no or little catalyst deactivation was observed over low Ni-loaded catalysts (Figure 7d). To reveal the active site for the formation of C_2H_4, the SM sample, including Mg instead of Ni, was used for the steam reforming of ethanol. A C_2H_4 selectivity of 96% was observed at a conversion of 6.5%. Therefore, we conclude that the dehydration of ethanol is likely to occur on the SM support, and this can also explain the increase of the selectivity to C_2H_4 as the Ni loading is reduced. Nishiyama and Shirai [28,29] measured FTIR spectra of pyridine adsorbed on smectites and indicated the presence of weak Lewis acid sites and the absence of Brønsted ones, and hence, these acidic properties of the smectite surface induced the dehydration of ethanol, but not for the decomposition of C_2H_4, for which the strong acid sites are needed [30–32]. It is noteworthy that the formation of C_2H_4 was not observed during the reaction over SM(Ni35), whereas the selectivity to C_2H_4 gradually increased over Ni35/SM (Figure 7d). These results indicate that the Ni-containing smectite structure is useful for the suppression of the side reaction of ethanol to C_2H_4 and contributes to the increase of the selectivity to the steam reforming reaction. These features of Ni-containing smectite materials would be beneficial for other catalytic reactions, in which the carbon deposition and/or the dehydration should be avoidable.

3. Experimental Section

3.1. Catalyst Preparation

Smectite materials were prepared in the same manners as described elsewhere [17,18]. Aqueous solutions of water glass (Nippon Chemical, Tokyo, Japan) and NaOH (Wako Pure Chemical, Osaka, Japan) were mixed, and an aqueous solution of $MgCl_2$ (Wako) was dropped into the mixed solution until the molar ratio of Si/Mg became 8/6 while stirring. After stirring for 12 h under ambient conditions, the resultant solid material was separated by filtration and washed with distilled water. The solid material was put into a certain volume of water (20 cm^3), of which the pH was 7.34, and the slurry obtained was put into a stainless steel autoclave (100 cm^3). After a heat treatment at 150 °C for 2 h, the solid material produced was separated by filtration and washed with distilled water, dried at 80 °C overnight and calcined at 300 °C for 1 h. Nickel-containing smectite material was also prepared with similar procedures using $NiCl_2$ (Wako) instead of $MgCl_2$, in which the amount of Ni included was 35 wt %. The SM(Ni) sample was reduced in a stream of 4% H_2 in N_2 at a rate of 50 $cm^3 \cdot min^{-1}$ and at increasing temperatures at a rate of 10 $K \cdot min^{-1}$ up to 700 °C, at which it was further reduced for 1 h. SM-supported Ni catalyst was prepared by the impregnation method. The material was impregnated with an aqueous solution of $Ni(NO_3)_2 \cdot 6H_2O$ (Wako) at 70 °C under reduced pressure, dried at 110 °C overnight and calcined at 500 °C for 3 h. The loadings of Ni prepared were 5, 10 and 35 wt %. SiO_2 (GL Science, Tokyo, Japan), Al_2O_3 (Catalysis Society of Japan, JRC-ALO4) and MgO (Kishida Chemical, Osaka, Japan) were also used for supports, and Ni was loaded onto these supports in 35 wt % by impregnation using $NiCl_2$.

3.2. Catalyst Characterization

Total surface area was measured by nitrogen adsorption at −196 °C on Quantachrome NOVA 1200 (Version 7.01). The samples were pretreated by evacuation at 150 °C for 2 h. The structural properties

of Ni species before and after reduction were examined by X-ray diffraction (XRD) on a JEOL JDX-8020 with Ni-filtered CuKα radiation. The crystallite size of Ni was determined by Scherrer's equation. The area of exposed Ni species was measured by CO pulse chemisorption (BEL Japan BEL-METAL, Osaka, Japan) at 50 °C using a pulse of 5% CO in He. Prior to the chemisorption, the samples were treated in a stream of 5% H_2 in He at 600 °C for 1 h.

3.3. Steam Reforming of Ethanol

The steam reforming of ethanol was carried out in a glass fixed-bed flow reactor at atmospheric pressure. A catalyst sample (0.01 g) was placed in the reactor, reduced in a stream of 4% H_2 in N_2 at a rate of 50 $cm^3 \cdot min^{-1}$ and at increasing temperatures up to 600 °C and further reduced at this temperature for 1 h. After cooling to room temperature in N_2, the reactor was heated to a reaction temperature of 500 °C. A mixture of ethanol and water diluted with N_2, of which the partial pressures were 0.05 and 0.15 atm, respectively, was introduced at a total flow rate of 200 $cm^3 \cdot min^{-1}$. All of the products after the reaction were analyzed by gas chromatographs with thermal conductivity detector (TCD) and flame ionization detector (FID). The total conversion of ethanol was determined from the concentration measured before and after reaction. The selectivity to the carbon-containing products was determined on the carbon basis, and the selectivity to CO_2 was used as a measure of the selectivity to the desired steam reforming of ethanol. The H_2 yield was determined from the amount of H_2 formed divided by the stoichiometric maximum amount of H_2 in the steam reforming of ethanol (Equation (1)) to be obtained under the conditions used.

3.4. Estimation of Carbon Deposition

The amount of carbon deposited on the surface of Ni catalysts was determined as follows. A used catalyst sample was subjected to the thermal treatment in a stream of 4% H_2 in N_2 at a rate of 100 $cm^3 \cdot min^{-1}$ and at increasing temperatures up to 700 °C and at this temperature for a few hours. The total amount of CH_4 evolved during the treatment was measured.

4. Conclusions

The stability of Ni catalyst for the steam reforming of ethanol was improved by the use of a Ni-containing smectite-derived material as a precursor. The decomposition of CO and CH_4 to the carbon deposition on Ni particles causes significant catalyst deactivation, but it can be suppressed to an even larger extent for the Ni-containing smectite-derived catalyst. Furthermore, the side reaction of the dehydration of ethanol to C_2H_4, which occurs on the acid sites of the support, was completely inhibited. The smectite-derived catalyst contains smaller and more stable Ni crystallites compared to other conventional supported Ni catalysts, which should be related to the formation of exposed Ni crystallites from the smectite bulk structure, different from that via impregnation, in which Ni is loaded onto support materials from outside.

Author Contributions

Experimental works on the preparation of catalysts and their activity test were mainly done by Ryohei Yamaoka under guidance of Hiroshi Yoshida and Masahiko Arai. The reaction and catalyst characterization results were analyzed and discussed by all the authors and the manuscript was mainly prepared by Hiroshi Yoshida in cooperation with Masahiko Arai.

Conflicts of Interest

The authors declare no conflict of interest

References

1. Navarro, R.M.; Peña, M.A.; Fierro, J.L.G. Hydrogen production reactions from carbon feedstocks: Fossil fuels and biomass. *Chem. Rev.* **2007**, *107*, 3952–3991.
2. Katikaneni, S.P.; Al-Muhaish, F.; Harale, A.; Pham, T.V. On-site hydrogen production from transportation fuels: An overview and techno-economic assessment. *Int. J. Hydrog. Energy* **2014**, *39*, 4331–4350.
3. Freni, S.; Cavallaro, S.; Mondello, N.; Spadaro, L.; Frusteri, F. Production of hydrogen for MC fuel cell by steam reforming of ethanol over MgO supported Ni and Co catalysts. *Catal. Commun.* **2003**, *4*, 259–268.
4. Mariño, F.; Baronetti, G.; Jobbagy, M.; Laborde, M. Cu-Ni-K/γ-Al_2O_3 supported catalysts for ethanol steam reforming: Formation of hydrotalcite-type compounds as a result of metal-support interaction. *Appl. Catal. A Gen.* **2003**, *238*, 41–54.
5. Sun, J.; Qiu, X.P.; Wu, F.; Zhu, W.T. H_2 from steam reforming of ethanol at low temperature over Ni/Y_2O_3, Ni/La_2O_3 and Ni/Al_2O_3 catalysts for fuel-cell application. *Int. J. Hydrog. Energy* **2005**, *30*, 437–445.
6. Muroyama, H.; Nakase, R.; Matsui, T.; Eguchi, K. Ethanol steam reforming over Ni-based spinel oxide. *Int. J. Hydrog. Energy* **2010**, *35*, 1575–1581.
7. Iulianelli, A.; Liguori, S.; Longo, T.; Tosti, S.; Pinacci, P.; Basile, A. An experimental study on bio-ethanol steam reforming in a catalytic membrane reactor. Part II: Reaction pressure, sweep factor and WHSV effects. *Int. J. Hydrog. Energy* **2010**, *35*, 3159–3164.
8. Song, H.; Zhang, L.; Ozkan, U.S. Effect of synthesis parameters on the catalytic activity of Co-ZrO_2 for bio-ethanol steam reforming. *Green Chem.* **2007**, *9*, 686–694.
9. Machocki, A.; Denis, A.; Grzegorczyk, W.; Gac, W. Nano- and micro-powder of zirconia and ceria-supported cobalt catalysts for the steam reforming of bio-ethanol. *Appl. Surf. Sci.* **2010**, *256*, 5551–5558.
10. Kazama, A.; Sekine, Y.; Oyama, K.; Matsukata, M.; Kikuchi, E. Promoting effect of small amount of Fe addition onto Co catalyst supported on α-Al_2O_3 for steam reforming of ethanol. *Appl. Catal. A Gen.* **2010**, *383*, 96–101.
11. Liguras, D.K.; Kondarides, D.I.; Verykios, X.E. Production of hydrogen for fuel cells by steam reforming of ethanol over supported noble metal catalysts. *Appl. Catal. B Environ.* **2003**, *43*, 345–354.

12. Frusteri, F.; Freni, S.; Spadaro, L.; Chiodo, V.; Bonura, G.; Donato, S.; Cavallaro, S. H_2 production for MC fuel cell by steam reforming of ethanol over MgO supported Pd, Rh, Ni and Co catalysts. *Catal. Commun.* **2004**, *5*, 611–615.
13. Erdőhelyi, A.; Raskó, J.; Kecskés, T.; Tóth, M.; Dömök, M.; Baán, K. Hydrogen formation in ethanol reforming on supported noble metal catalysts. *Catal. Today* **2006**, *116*, 367–376.
14. Birot, A.; Epron, F.; Descorme, C.; Duprez, D. Ethanol steam reforming over $Rh/Ce_xZr_{1-x}O_2$ catalysts: Impact of the $CO\text{-}CO_2\text{-}CH_4$ interconversion reactions on the H_2 production. *Appl. Catal. B Environ.* **2008**, *79*, 17–25.
15. Christensen, K.O.; Chen, D.; Lødeng, R.; Holmen, A. Effect of supports and Ni crystal size on carbon formation and sintering during steam methane reforming. *Appl. Catal. A Gen.* **2006**, *314*, 9–22.
16. Torii, K.; Iwasaki, T. Synthesis of novel Ni-hectorite inorganic complexes. *Chem. Lett.* **1988**, *17*, 2045–2048.
17. Arai, M.; Guo, S.-L.; Shirai, M.; Nishiyama, Y.; Torii, K. The catalytic activity of platinum-loaded porous smectite-like clay minerals containing different divalent cations for butane hydrogenolysis and ethylene hydrogenation. *J. Catal.* **1996**, *161*, 704–712.
18. Arai, M.; Kanno, M.; Nishiyama, Y.; Torii, K.; Shirai, M. Synthetic smectite-like materials containing different divalent cations as catalysts and supports for gas-phase hydrogenation of acetonitrile. *J. Catal.* **1999**, *182*, 507–510.
19. Bhanage, B.M.; Fujita, S.; Ikushima, Y.; Torii, K.; Arai, M. Synthesis of dimethyl carbonate and glycols from carbon dioxide, epoxides and methanol using heterogeneous Mg containing smectite catalysts: effect of reaction variables on activity and selectivity performance. *Green Chem.* **2003**, *5*, 71–75.
20. Fujita, S.; Bhanage, B.M.; Aoki, D.; Ochiai, Y.; Iwasa, N.; Arai, M. Mesoporous smectites incorporated with alkali metal cations as solid base catalysts. *Appl. Catal. A Gen.* **2006**, *313*, 151–159.
21. Iwasa, N.; Yamane, T.; Arai, M. Influence of alkali metal modification and reaction conditions on the catalytic activity and stability of Ni containing smectite-type material for steam reforming of acetic acid. *Int. J. Hydrog. Energy* **2011**, *36*, 5904–5911.
22. Iwasa, N.; Takizawa, M.; Arai, M. Preparation and application of nickel-containing smectite-type clay materials for methane reforming with carbon dioxide. *Appl. Catal. A Gen.* **2006**, *314*, 32–39.
23. Yoshida, H.; Watanabe, K.; Iwasa, N.; Fujita, S.; Arai, M. Selective methanation of CO in H_2-rich gas stream by synthetic nickel-containing smectite based catalysts. *Appl. Catal. B Environ.* **2015**, *162*, 93–97.
24. Fujita, S.; Yamanishi Y.; Arai, M. Synthesis of glycerol carbonate from glycerol and urea using zinc-containing solid catalysts: A homogeneous reaction. *J. Catal.* **2013**, *297*, 137–141.
25. Fujita, S.; Tanaka, M.; Arai, M. Synthesis of quinazoline-2,4(1H,3H)-dione from carbon dioxide and 2-aminobenzonitrile using mesoporous smectites incorporated with alkali hydroxide. *Catal. Sci. Technol.* **2014**, *4*, 1563–1569.
26. Vicente, J.; Montero, C.; Ereña, J.; Azkoiti, M.J.; Bilbao, J.; Gayubo, A.G. Coke deactivation of Ni and Co catalysts in ethanol steam reforming at mild temperatures in a fluidized bed reactor. *Int. J. Hydrog. Energy* **2014**, *39*, 12586–12596.

27. Vicente, J.; Ereña, J.; Montero, C.; Azkoiti, M.J.; Bilbao, J.; Gayubo, A.G. Reaction pathway for ethanol steam reforming on a Ni/SiO_2 catalyst including coke formation. *Int. J. Hydrog. Energy* **2014**, *39*, 18820–18834.
28. Nishiyama, Y.; Arai, M.; Guo, S.-L.; Sonehara, N.; Naito, T.; Torii, K. Catalytic properties of hectorite-like smectites containing nickel. *Appl Catal. A Gen.* **1993**, *95*, 171–181.
29. Shirai, M.; Aoki, K.; Torii, K.; Arai, M. Acidity and 1-butene isomerization of synthesized smectite-type catalysts containing different divalent cations. *Appl. Catal. A Gen.* **1999**, *187*, 141–146.
30. Rostrup-Nielsen, J.R.; Hojlund, N. *Deactivation and Poisoning of Catalyst*; Oudar, J., Wise H., Dekker, M.. eds; CRC Press: Boca Raton, FL, USA, 1985; p. 57.
31. Aupretre, F.; Descorme, C.; Duprez, D.; Casanave, D.; Uzio, D. Ethanol steam reforming over $Mg_xNi_{1-x}Al_2O_3$ spinel oxide-supported Rh catalysts. *J. Catal.* **2005**, *233*, 464–477.
32. Vizcaíno, A.J.; Carrero, A.; Calles, J.A. Hydrogen production by ethanol steam reforming over Cu-Ni supported catalysts. *Int. J. Hydrog. Energy* **2007**, *32*, 1450–1461.